DEVELOPMENT OF A NEW COMPUTER PROGRAM FOR DYNAMIC AND STATIC PILE LOAD TESTS

T. Wakisaka [i)], T. Matsumoto [ii)], E. Kojima [iii)] & S. Kuwayama [iii)]

ABSTRACT It has been believed that the static load test is the most reliable method to obtain the load-settlement relation of a pile. Most static load tests are conducted using reaction piles as the reaction system. However, some researches point out that the influence of the reaction piles on the measured load-settlement relation may not be neglected, and that an analysis of the measured data is required to obtain a true load-settlement of the. From this point of view, the dynamic load testing or the rapid load testing may not be necessarily inferior to the static load test, considering cost and time performance of the dynamic load test as well. In this study, a new computer program for analysing the stress-wave propagation phenomena in pile driving was developed using a finite difference scheme and rational soil resistance models. Verification analyses of the proposed method are conducted first, and then the developed method is applied to the dynamic and static load tests on an end-bearing concrete pile.

Keywords: pile driving analysis, static analysis, finite difference, wave-propagation equation,

1. INTRODUCTION

To obtain the load-settlement relation of a pile, it has been believed that the static axial load test is the most reliable method. Most static load tests are conducted using reaction piles as the reaction system. However, Latozle *et al*. (1997), Poulos (1998) and Kitiyodom, Matsumoto & Kanefusa (2004) suggest that the influence of the reaction piles on the measured load-settlement relation may not be neglected, and that an analysis of the measured data is required to obtain a true load-settlement of the pile.

The dynamic load testing and the rapid load testing are unsusceptible to reaction piles. The dynamic load testing requires less time and cost compared to the rapid load testing. Thus, the dynamic load testing can be applied to many piles in a construction site to determine the distribution of pile capacity that could be used in reliability design of the pile foundation (Hayashi, Matsumoto & Suzuki 2000).

Several computer programs for analysing the one-dimensional wave propagation in a pile have been developed, such as Smith method (Smith 1960), WEAP (Goble & Rausche 1976), CAPWAP (Rausche et al. 1972), TNOWAVE (TNO 1977), KWAVE (Matsumoto & Takei 1991) and others. Recently, analytical methods based on the characteristic solutions of the one-dimensional wave equation without skin friction may be prevailing. The characteristic method treats skin frictions as discrete concentrated forces, and deals with them as external forces acting along the pile shaft. In the authors' experience, the calculation using the characteristic method tends to oscillate or diverge when very large values of the soil stiffness or the damping are encountered. Recently in Japan, impact force applied to a test pile sometimes reaches the point that near the yield stress of the pile. In such pile driving, non-linearity of the pile material, especially for concrete piles, would be taken into account in the wave propagation analysis.

In this study, a numerical method for the one-dimensional wave equation in which the shaft resistance of the pile is explicitly considered was developed using finite difference scheme. The proposed method is incorporated in a computer program KWAVEFD. The program can consider changes in the pile section and non-linearity of the pile material. Furthermore, the program can be also used to calculate the static load-settlement relation of a pile.

In order to examine the validity of the newly developed program, verification analyses were conducted, and responses of the incorporated soil models are demonstrated first. Then the program is applied to the static and dynamic load tests of an end-bearing concrete pile.

i) Graduate student, Graduate School of Kanazawa University, Kanazawa, Japan
ii) Professor, Department of Civil Engineering, Kanazawa University, Kanazawa, Japan
iii) Geotop Corporation, Tokyo, Japan

2. THEORETICAL BASIS

2.1 Finite difference approximation of wave equation

In the proposed method, the differential equation (Eq. (1)) for the one-dimensional wave propagation in a pile is solved by means of a finite difference scheme.

$$\frac{\partial^2 w}{\partial t^2} = c^2 \frac{\partial^2 w}{\partial x^2} + H\tau, \quad H = -\frac{1}{\rho}\frac{2}{r} \qquad (1)$$

in which, t is the time, x the coordinate along the pile axis, c the wave velocity, τ skin friction, and w, r, ρ are the displacement, the radius and the density of the pile, respectively. In Eq. (1), the influence of skin friction (or end resistance) is explicitly considered, unlike the characteristic solutions of the wave equation.

Finite difference approximation for Eq. (1) is expressed by Eq. (2) to take into account a change in pile section properties shown in Fig. 1.

$$w_{i,j+1} = 2w_{i,j} - w_{i,j-1}$$
$$+ \frac{2}{(A_i \rho_i + A_{i+1}\rho_{i+1})}\left(\frac{\Delta t}{\Delta x}\right)^2 \times$$
$$(A_{i+1}E_{i+1}w_{i+1,j} - A_i E_i w_{i,j} - A_{i+1}E_{i+1}w_{i,j} + A_i E_i w_{i-1,j})$$
$$- \frac{U_i + U_{i+1}}{A_i \rho_i + A_{i+1}\rho_{i+1}}(\Delta t)^2 \tau_{i,j} \qquad (2)$$

where Δt is the time increment, A is the cross-sectional area, E the Young's modulus, U the circumferential length of a pile element having a length of Δx. Subscripts 'i' and 'j' denote node number and time step, respectively.
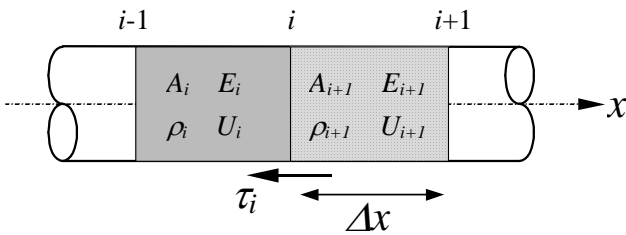

Figure 1. Notations used

2.2 Soil models

Figure 2 shows the shaft resistance model incorporated into KWAVEFD. The values of the shaft spring, k_s, and the radiation damping, c_r, per unite area are approximately obtained from the work of Novak $et\ al.$ (1978) as follows:

$$k_s = \frac{2.75G}{2\pi r}, \quad c_r = \frac{G}{V_s} \qquad (3)$$

where G and V_s are the shear modulus and the shear wave velocity of the surrounding soil respectively.

The dynamic friction, τ_d, is generally taken as a non-linear function of velocity, according to

$$\tau_d = \tau_{max}\left\{1 + \alpha\left(\frac{\Delta v}{v_0}\right)^\beta\right\} \qquad (4)$$

where τ_{max} is the static maximum shaft friction, v_0 is a reference velocity (taken for convenience as 1 m/s), and Δv is the relative velocity between the pile and the adjacent soil. Non-linear viscous laws similar to Eq. (4) have been proposed by Gibson and Coyle (1968), Heerema (1979) and Litkouhi and Poskitt (1980), all of whom suggest a value of β close to 0.2, with the parameter α varying from about 0.1 for sand, to unity for clay soils (after Randolph & Deeks 1992). The relation of Eq. (4) was introduced into the viscous damping in Fig. 2.
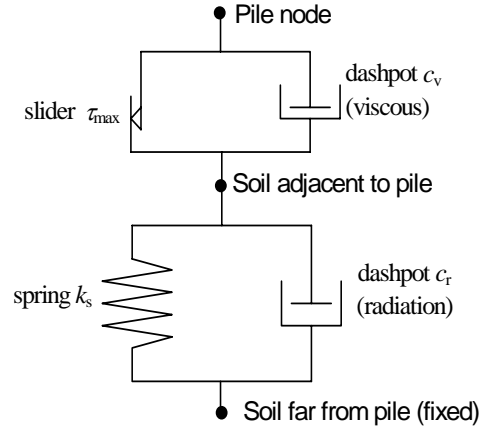

Figure 2. Shaft resistance model
(after Randolph & Simons, 1986)

Figure 3 shows the pile base resistance model. The value of the soil spring, k_b, the damping, c_b ($c_{b1} = c_{b2}$), and the lumped soil mass, m_b, per unit base area can be estimated as follows (Deeks & Randolph 1993):

$$k_b = \frac{4G}{\pi r(1-\nu)}, \quad c_b = \frac{3.4}{\pi(1-\nu)}\frac{G}{V_s},$$
$$m_b = 16r\frac{0.1 - \nu^4}{\pi(1-\nu)}\rho_s \qquad (5)$$

where ν and ρ_s are the Poisson's ratio and the density of the soil respectively.

Non-linear response of the soil spring at the pile base can be taken into account, based on an empirical relation of Eq. (6) (Chow 1986).

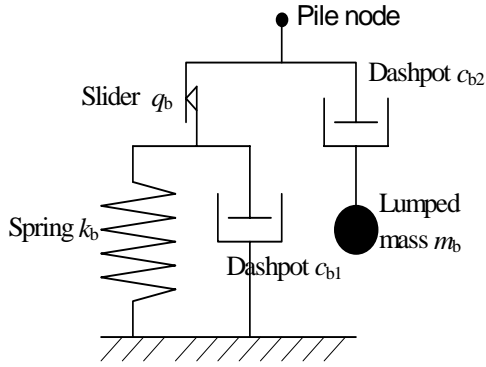$$k_b = \left(1 - R_f \frac{q}{q_b}\right)k_{b0} \qquad (6)$$

2

Figure 3. Pile base resistance model
(after Deeks & Randolph, 1995)

In Eq. (6), R_f is the reduction coefficient, q is the static base stress (stress in the spring), q_b is the static ultimate base resistance, and k_{b0} is the initial spring stiffness.

The typical response of the non-linear soil spring is illustrated in Figure 4. The soil spring response in unloading and reloading stages is modelled as linear having the stiffness of k_{b0}.

The program KWAVEFD can be used for estimating the pile and soil behaviours subjected to static, rapid and dynamic loading.
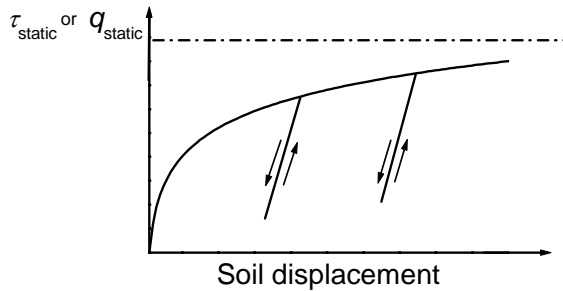
Figure 4. Non-linear soil model

3. VERIFICATION ANALYSES

3.1 Comparison to theoretical values

The wave equation free from the skin friction has the theoretical solutions. Therefore, impacts on a homogeneous pile and a non-homogeneous pile without soil resistance are calculated by the program KWAVEFD, and the calculated results are compared with the theoretical values in below.

3.1.1 Homogeneous pile

Table 1 shows the specifications of a homogeneous pile to be analysed here.

Figure 5 shows the impact stress applied to the pile head. Figure 6 shows the calculated and theoretical distributions of axial stresses along the pile. Theoretically, the front of compression stress reaches the pile base at $t = 2$ ms because the wave

velocity is 5000 m/s. The compression stress is reflected at the pile base, and it goes back to the pile head as the tension stress and reaches the pile head at $t = 4$ ms. The calculated results are in good agreements with these theoretical solutions. Figure 7 shows the time vs. pile displacement at the middle point ($x = 5$ m). A good agreement between the theoretical and calculated values can be seen again.

Table 1. Specifications of homogeneous pile

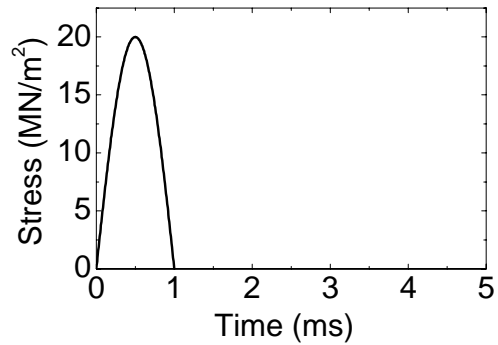| Length (m)	10
Diameter (mm)	400
Cross-sectional area (m^2)	0.126
Young's modulus (kN/m^2)	3.0×10^7
Wave velocity (m/s)	5000
Density (ton/m^3)	1.2
Mass (ton)	1.51

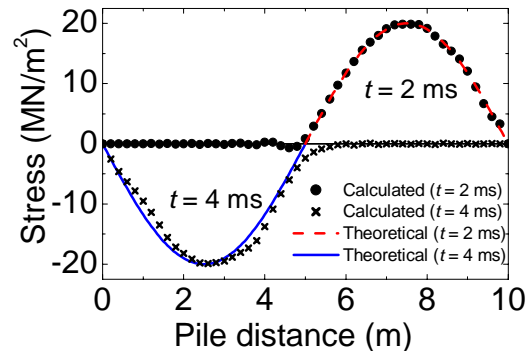Figure 5. Pile head stress

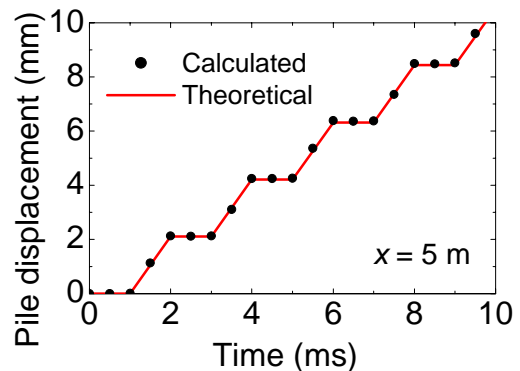Figure 6. Distributions of the stresses in the pile

Figure 7. Time vs. pile displacement

3

3.1.2. Non-homogeneous pile

A non-homogeneous pile with no soil resistance shown in Table 2 was also analysed using the proposed method. The pile consists of two sections having the same material but different cross-sectional areas; the cross-sectional area of the lower section is twice the upper section. The impact stress shown in Figure 5 was used in this analysis again.

Figures 8 and 9 show time vs. velocity and time vs. displacement at the pile head, respectively. Good agreements between the calculated and theoretical results can be seen in both the velocity and displacement.

Table 2. Specifications of non-homogeneous pile

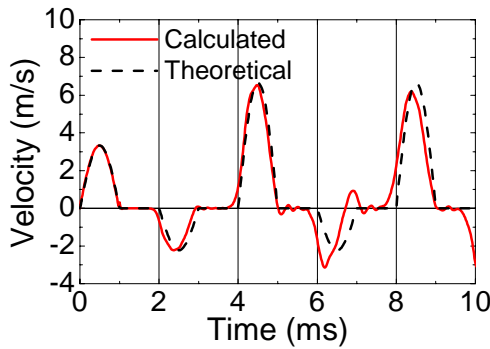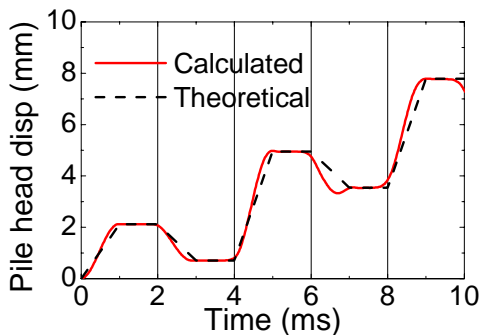|	Upper	Lower
Length (m)	5	5
Diameter (mm)	100	141.4
Cross section area (m^2)	7.85×10^{-3}	15.7×10^{-3}
Young's modulus (kN/m^2)	3.0×10^7	3.0×10^7
Wave velocity (m/s)	5000	5000
Density (ton/m^3)	1.2	1.2

Figure 8. Time vs. pile head velocity

Figure 9. Time vs. pile head displacement

3.2 Friction pile with elastic soil response

It is known that the one-dimensional wave equation considering skin friction has no theoretical solutions. Hence, a perfect friction pile without base resistance with elastic firction response is analysed, and the calculated results are compared with the theoretical solutions of the single mass system shown in Figure 10.

$M_h = 1.51$ ton
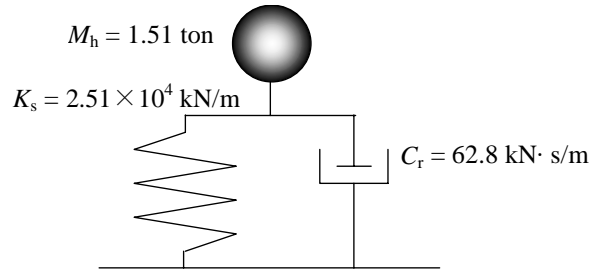$K_s = 2.51 \times 10^4$ kN/m
$C_r = 62.8$ kN· s/m

Figure 10. Single mass system

Specifications of the pile to be analysed here are the same as Table 1. The values of the shaft spring stiffness, k_s, and the radiation damping, c_r, were set as $k_s = 2.0 \times 10^3$ kN/m^3 and $c_r = 5.0$ kN· s/m^3 along the pile shaft uniformly for convenience. The corresponding values of the total spring stiffness, K_s, and the total damping, C_r, in the single mass system are shown in Fig. 10.

Figures 11 and 12 show time vs. displacement of the middle point of the pile without damping ($c_r = 0$) and with damping, respectively. Overall, the calculated results are in good agreements with the theoretical solutions in both cases. Periodical oscillations having a period of $2L/c$ can be seen in the calculated results, which are never seen in the theoretical solutions. It is interesting to note that these oscillations in the calculation results reflect the wave propagation phenomena in the pile, which cannot be simulated using the single mass system.
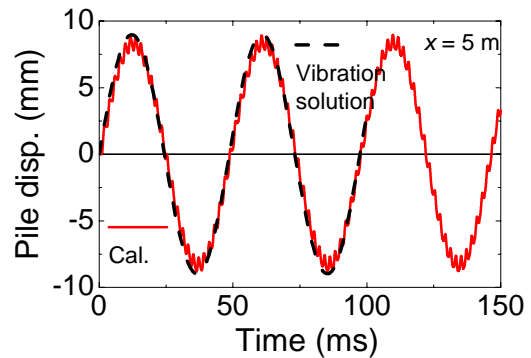

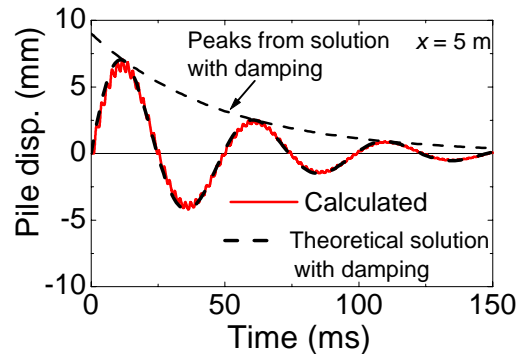Figure 11. Time vs. pile disp. (without damping)

Figure 12. Time vs. pile disp. (with damping)

4

3.3 Responses of soil resistance models

To demonstrate the responses of the soil models (Figures 2 and 3), analyses of pile driving on a perfect friction pile and a perfect end-bearing pile were carried out separately. The specifications of the pile are the same as Table 1. The soil parameters and the corresponding values of the soil resistance models are summarised in Table 3. The bi-linear response ($R_f = 0$) was assumed for the soil springs. The impact stress shown in Fig. 5 was applied to the top of both piles.

Three types of pile driving analysis were conducted for each pile. In the analyses of the perfect friction pile, k_s alone was considered in Type F1, k_s and c_r in Type F2, and k_s, c_r, α and β in Type F3, in order to demonstrate the effect of each component. In the analyses of the perfect end-bearing pile, k_b alone was considered in Type B1, k_b and c_{b1} in Type B2, and k_b, c_{b1} and c_{b2} (i.e. M_b) in Type B3.

Table 3. Soil resistance parameters

Soil		
	G (kN/m^2)	5000
	v_s	0.5
	ρ_s (ton/m^3)	1.8
Shaft resistance (in perfect friction pile)	τ_s (kN/m^2)	30
	k_s (kN/m^3)	10942
	c_r (kN·s/m^3)	94.9
	α	1.0
	β	0.2
Base resistance (in perfect end-bearing pile)	q_b (kN/m^2)	600
	k_b (kN/m^3)	6.35×10^4
	c_b (kN·s/m^3)	205.3
	M_b (ton)	0.017

Figure 13 shows the mobilisations of the shaft resistance at the middle point of the pile ($x = 5$ m) calculated from Types F1, F2 and F3. It can be seen that the separation of the pile and the adjacent soil and re-join of them are well simulated. It is also seen that the effects of the radiation damping, c_r, and the dependency of the dynamic shaft resistance on the relative velocity between the pile and the adjacent soil after yielding (i.e. effects of α and β) are well simulated.

Figure 14 shows the time vs. pile displacement calculated from Type F3. The displacements of the pile and the soil are calculated separately after the yielding. The rebound of the pile as well as the soil are simulated well.

Figure 15 shows the mobilisations of the base resistance calculated from Types B1, B2 and B3. It is seen that the effects of the radiation damping (c_{b1}) and the lumped soil mass (c_{b2} and M_b) are well simulated and that these effects are very large in pile driving.
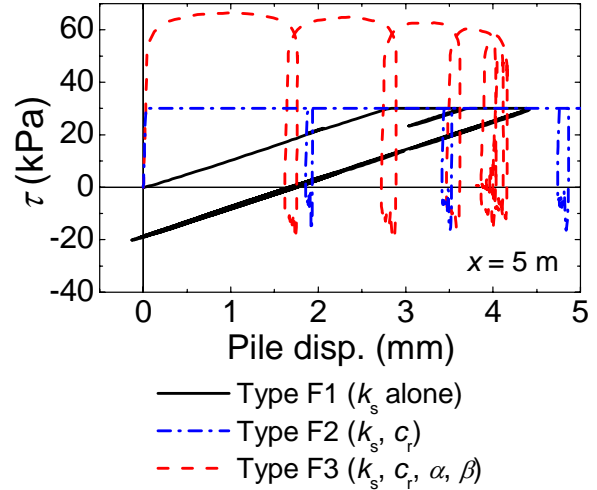

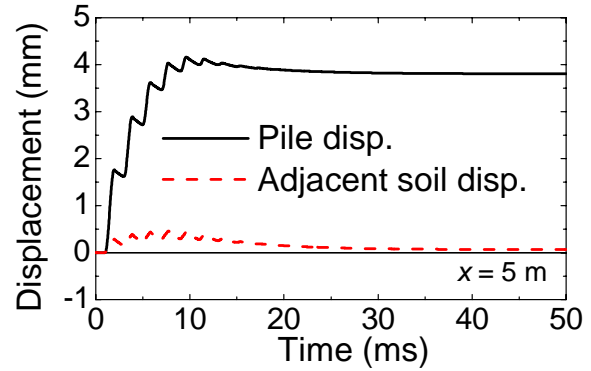Figure 13. Mobilisation of the shaft resistance
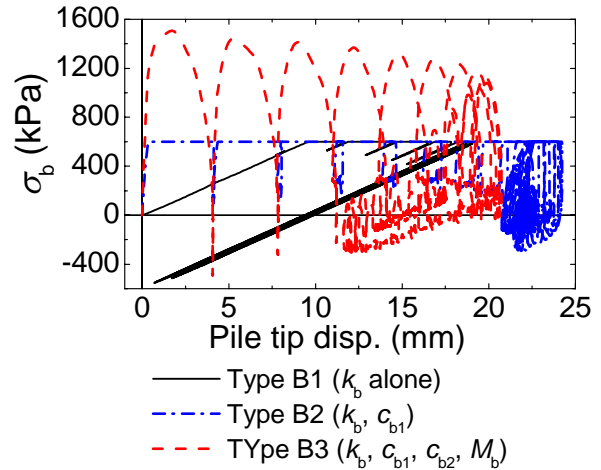

Figure 14. Time vs displacements

Figure 15. Mobilisation of the pile base resistance

4. APPLICATION TO AN ACTUAL END-BEARING CONCRETE PILE

The newly developed program KWAVEFD was applied to the static and dynamic load tests of an actual end-bearing pile carried out by Kojima & Kuwayama (2003).

4.1 Test description

The test pile was a concrete pile, 8 m long and 400 mm diameter. The specifications of the test pile are shown in Table 4. The test pile was inserted in a pre-installed steel pile casing having an inner diameter of 580 mm (Fig. 16). A rubber membrane, 40 mm thickness, was placed beneath the pile base, making the test pile a perfect end-bearing pile. Below the rubber membrane was a relatively hard soil having the SPT blow count, N, of 15.

The static load test of the pile was carried out prior to the dynamic load tests. The relationship between the load and the pile base displacement is shown in Fig. 17. A linear relationship between them was observed until the pile head load of 30 kN. From this result, the value of k_b was estimated, and the corresponding values of the shear modulus, G, of the ground (the rubber membrane in this particular test) and c_b were calculated using the relations in Eq. (4) with assumptions of the Poisson's ratio $\nu = 0.3$ and the soil density $\rho_s = 1.8$ ton/m^3 for the first approximations to be used in the wave matching analysis (Table 5).

In the dynamic load tests, the pile was driven by falling a hammer mass of 0.3 ton onto the pile head. Strains and accelerations were measured at $x_m = 0.9$ m below the pile head with a sampling rate of 15 μs.

Table 4. Specifications of the test pile

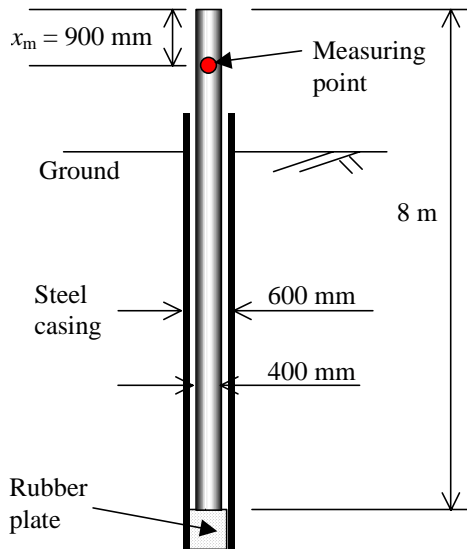| Length (m)	8
Outer diameter (mm)	400
Inner diameter (mm)	270
Cross-sectional area (cm^2)	684.1
Young's modulus (kN/m^2)	3.92×10^7
Wave velocity (m/s)	4636
Density (ton/m^3)	1.825
Pile mass (ton)	1.0

Figure 16. Illustration of the set pile

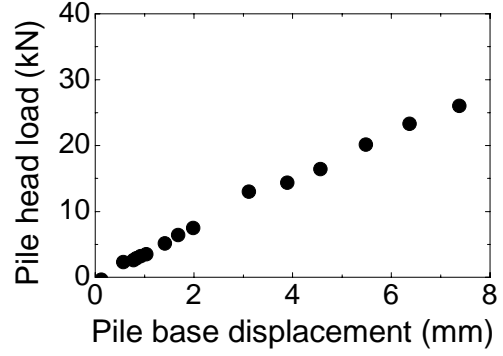
Figure 17. Result of the static load test

Table 5. Soil parameters (initial values)

Spring stiffness, k_b (kN/m^3)	5.12×10^4
Shear modulus, G (kN/m^2)	9.42×10^3
Damping, c_b (kN·s/m^3)	201.4
Added mass, m_b (ton/m^2)	0.31
Maximum base resistance, q_b (kN/m^2)	1200

4.2 Matching analyses of dynamic load tests

In the first pile driving test, the falling height of the hammer was 1.1 m. The impact force on the pile head is shown in Figure 18. The impact force, $F(0, t)$, was obtained from the downward and upward travelling forces, F_d and F_u, measured at the measuring point of $x_m = 0.9$ m.

$$F(0,t) = F_d\left(x_m, t - \frac{x_m}{c}\right) + F_u\left(x_m, t + \frac{x_m}{c}\right) \quad (7)$$

The impact force in Fig. 18 was used as the boundary condition at the pile head in the pile driving analysis.

Figure 19 shows the results of the initial matching analysis of the first driving. The soil resistance parameters listed in Table 5 were used in this analysis. Although periodic changes in the calculated force and velocity correspond to the measured results, their amplitudes overestimate the measured results of force and velocity due to underestimation of the radiation damping, c_b.
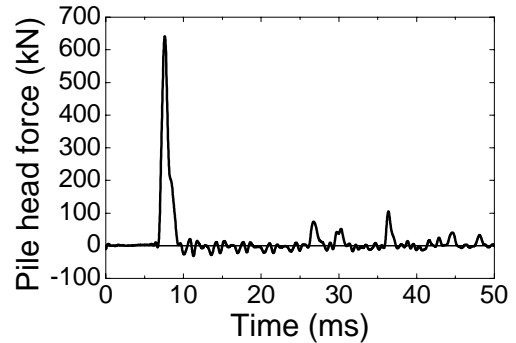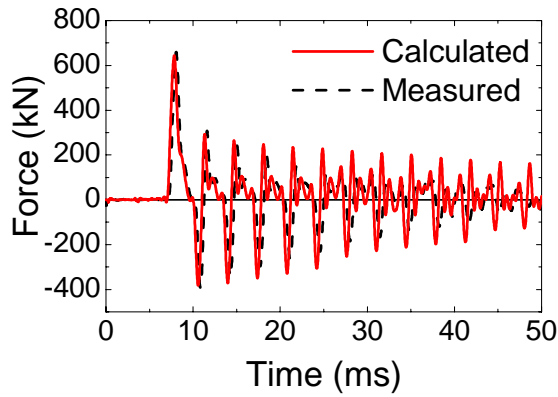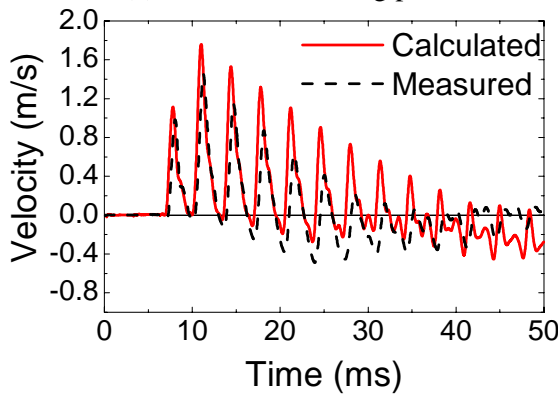

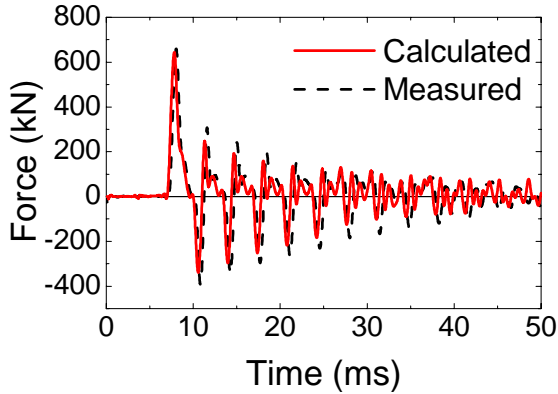Figure 18. Measured pile head force in the 1st driving
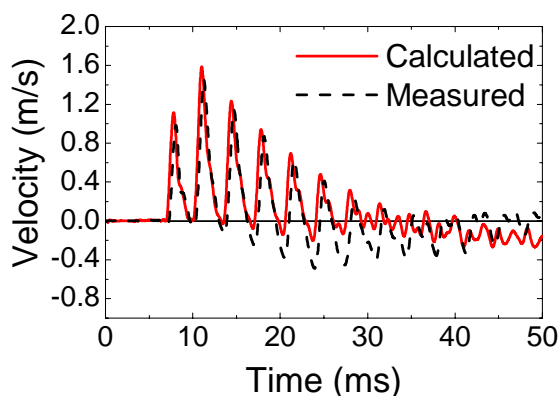
(a) Force at measuring point

(b) Velocity at measuring point
Figure 19. Results of initial matching analysis

(a) Force at measuring point

((b) Velocity at measuring point
Figure 20. Results of final matching analysis

Hence, matching analysis was proceeded changing the c_b value alone. The results of final matching analysis are shown in Fig. 20. In this analysis, $c_b = 415$ kN · s/m^3 was assumed. Remarkable agreements between the calculated and measured results in both of force and velocity were obtained. A larger value of the identified c_b compared to the initial assumption ($c_b = 201.4$ kN · s/m^3) may be attributed to the fact that the rubber membrane beneath the pile base was underlain by the hard soil as mentioned earlier.

4.3 Prediction analysis

The falling height of the hammer was reduced to 0.9 m in the second driving. The measured impact force in this driving is shown in Fig. 21. The stress at the measuring point was predicted using the same soil parameters identified in the final matching analysis of the first driving.

The predicted and measured forces at the measuring point are shown in Fig. 22. There is a good agreement between them, indicating the validity of the soil resistance parameters identified in the matching analysis of the first driving.
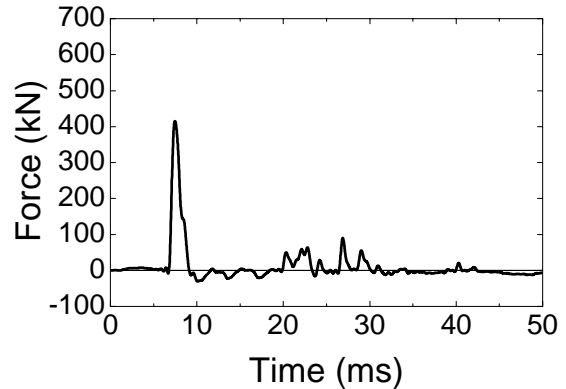

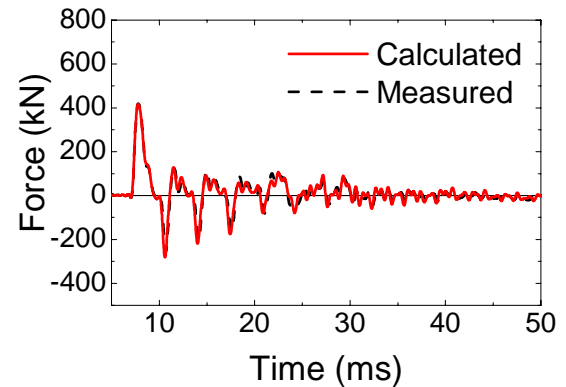Figure 21. Measured pile head force in the 2nd driving

Figure 22. Comparison of calculated and measured forces at the measuring point in the prediction analysis

7

4.4 Static analysis

KWAVEFD can be applied to not only the dynamic load test but also the static load test. In the static analysis, only loading rate on the pile head is decreased to an acceptable level so that the dynamic effects including wave propagation phenomena and soil damping can be negligible. The load-pile head settlement relation of the test pile was calculated using KWAVEFD and is compared with the measured one in Fig. 23. Good agreement was obtained as expected.
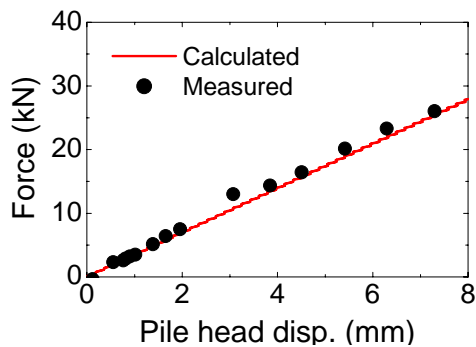

Figure 23. Static load test analysis

5. CONCLUDING REMARKS

A new numerical program KWAVEFD for analysing pile driving as well as static load test was developed in this study, based on the finite difference scheme. Rational soil resistance models have been incorporated in the program. Performance of the program was verified through comparisons with analytical solutions. Responses of the soil models were numerically demonstrated.

The developed program was applied to the dynamic and static load tests on a perfect end-bearing concrete pile. A good matching between the calculated and measured behaviour of the pile during driving was obtained. Then, the identified soil resistance parameters were used in prediction of the succeeding pile driving, and a good prediction was obtained. Furthermore, KWAVEFD was applied to the analysis of the static load test successfully.

REFERENCES

Chow, YK (1986). Analysis of vertically loaded pile groups. *Int. Jour. for Numerical and Analytical Methods in Geomech.*, **10**: 59-72.

Deeks AJ & Randolph MF (1995). A simple model for inelastic footing response to transient loading. *Int. Jour. for Num. and Analytical Methods in Geomech.*, **19**: 307-329.

Gibson G & Coyle H.M (1968). Soil damping onstant related to common soil properties in sands and clays. *Report No. 125-1,* Texas Transport Institute, Texas A & M University.

Goble G.G & Rausche F (1976). Wave equation analysis of pile driving-WEAP program, prepared for the U.S. department of transportation, federal highway administration, implementation division, office of research and development.

Hayashi, M., Matsumoto, T. & Suzuki, M. (2000). Dynamic load testing on 102 steel pipe piles for bridge foundations on mudstone. Proc. 6th Int. Conf. on the Application of Stress-Wave Theory to Piles, São Paulo, Brazil: 697 - 705.

Heerema E.P (1979). Relationships between wall friction, displacemen, velocity and horizontal stress in clay and in sand for pile driveability analysis. Ground Engineering, **12**(1).

Kitiyodom P, Matsumoto T & Kanefusa N (2004). Influence of reaction piles on the behaviour of test pile in static load testing. *Canadian Geotechnical Journal* (to be published).

Kojima E & Kuwayama S (2003). Development of a dynamic load test system on piles and its verification in experiments. *Proc. of the 48th Goetechnical Symposium,* JGS, Tokyo: 99-106.

Latotzke, J, König, D, and Jessberger, HL (1997). Effects of reaction piles in axial pile tests. *In Proc. of the 14th ICSMFE*, Hamburg, Germany, **2:** 097-1101.

Litkouhi S & Poskitt TJ (1980). Damping constant for pile driveability calculations. Geotechnique, **30**(1): 77-86.

Matsumoto, T & Takei, M. (1991). Effects of soil plug on behaviour of driven pipe piles, *Soil and Foundations* **3**(2): 14-34.

Novak M, Nogami T & Aboul-Ella F (1978). Dynamic soil reactions for plane strain case. *Jour. of Mechanical Eng. Div.*, ASCE **104**(EM4): 953-959.

Poulos HG (1998). Pile testing - From the designer's viewpoint. *Proc. of 2nd Int. Statnamic Seminar,* Tokyo, **1**: 3-21.

Randolph MF & Deeks AJ (1992). Dynamic and static soil models for axial pile response. *Proc. of 4th Int. Conf. on Application of Stress-Wave Theory to Piles,* The Hague: 3-14.

Randolph MF & Simons HA (1986). An improved soil model for one-dimensional pile driving analysis. *Proc. of the 3rd Int. Conf. on Numerical Methods in Offshore Piling*: 1-17.

Rausche F, Moses F & Goble G.G (1972). Soil resistance predictions from pile dynamics. *Jour. of the Soil Mech. and Found. Div., ASCE*, **98**(SM9).

Smith, E.A.L. (1960). Pile driving analysis of by the wave equation. *J. Soil Mech. and Found. Div., ASCE*, **86**(SM4): 35-61

TNO (1977). Dynamic pile testing. Report No. BI-77-13